

# Use of Experimental Designs to Evaluate the Influence of Methyl Green Dye as a Corrosion Inhibitor for Carbon Steel in Perchloric Acid

Tarik Attar<sup>1,2,\*</sup>, Abbas Benchadli<sup>2</sup>, Tayeb Mellal<sup>3</sup>, Boumediene Dali Youcef<sup>3</sup> and Esmachoukchou-Braham<sup>2</sup>

<sup>1</sup>Higher School of Applied Sciences of Tlemcen, BP 165, Bel Horizon, 13000 Tlemcen, Algeria

<sup>2</sup>Laboratory of Toxicomed, University Abou Beker Belkaid of Tlemcen, BP119, 13000 Tlemcen, Algeria

<sup>3</sup>Laboratory of Macromolecular Research (LRM), Department of Physics, Faculty of Sciences, University Abou Beker Belkaid of Tlemcen, BP119, 13000 Tlemcen, Algeria

\*Corresponding author (e-mail: att\_tarik@yahoo.fr, t.attar@essa-tlemcen.dz)

The aim of this research study was to apply experimental design in the optimization of influencing parameters on the corrosion inhibition efficiency of Methyl Green (MG) dye using the weight loss (WL) technique. Corrosion inhibition of carbon steel (CS) in the presence of different concentrations of MG dye in 1 M HClO<sub>4</sub> solution has been studied. Results showed that inhibition efficiency (IE) increased with increasing concentration of MG dye up to  $1.0 \times 10^{-3}$  mol/L, and decreased with raising temperature. The free energy values calculated from the Langmuir adsorption isotherm for MG dye (-36.24 to -38.04 kJ/mol) suggested that MG dye molecules adsorbed onto CS surface via a physicochemical mechanism.

**Key words:** Methyl Green dye; carbon steel; perchloric acid; thermodynamic and kinetic parameters; experimental design

*Received: August 2020; Accepted: October 2020*

Carbon steel is composed of a mixture of iron and carbon, accounting for about 85% of the total yearly steel production worldwide [1]. It is amply used in different industries, such as construction, marine, automotive, mining, and chemical processing industries, and petrochemical plants for applications involving alkaline, saline, and acidic environments due to its high mechanical properties, ready availability, and low cost.

Corrosion is a chemical or electrochemical process that gradually returns metal to its natural state in the environment. Corrosion inhibition is one of the great practical importance, being widely employed in reducing or stopping wastage of engineering materials and minimizing costs of corrosion control [2]. It employs chemical compounds that in small quantities can be used in processes to control metal dissolution [3, 4]. Organic compounds containing a heteroatom, such as oxygen, nitrogen, sulfur, and phosphorus, or containing double and triple bonds as well as aromatic rings are considered one of the most important materials recognized in practice and used as anti-corrosion inhibitors [5, 6].

The study of corrosion process and its inhibition by organic compounds, such as dyes, is a very active field of research in acidic or basic environments [7-13]. Dyes have long been applied in the coloring, printing, paper, leather, textile, plastics, cosmetic, medical, pharmaceutical, and agri-food industries, and in recent times as corrosion inhibitors

of metals and alloys in aggressive environments [14, 15].

Experimental design has been frequently used in the statistical optimization of analytical approaches because of its advantages such as reduction in the number of experiments that leads to the considerably less laboratory work and lower reagent consumption, as well as faster to implement and more cost effective than traditional one-at-a-time approach [16-20].

As a continuation of the studies on the use of organic dyes as corrosion inhibitors in acidic solutions, we have investigated the effect of Methyl Green dye on the corrosion inhibition of carbon steel in 1.0 M HClO<sub>4</sub> solution using weight loss and experimental design. The effects of concentration, temperature, and immersion time on inhibitor performance have been studied. The thermodynamic activation parameters for both dissolution and adsorption processes will be calculated and discussed.

## MATERIALS AND METHODS

### Material Preparation

The carbon steel used had the following composition (wt.%): C: 0.37%, Mn: 0.68%, Cu: 0.16%, Cr: 0.077%, Ni: 0.059%, Si: 0.023%, S: 0.016%, Ti: 0.011%, Co: 0.009%, and the remaining portion was Fe. Carbon steel samples were initially polished with emery paper (400, 800, and 1200) starting with coarse

until the mirror appearance was obtained and then washed with distilled water. They were cleaned again with acetone and finally dried using a hot air blower. The solution of 1 M HClO<sub>4</sub> was prepared by dilution of perchloric acid (70-72%, Sigma-Aldrich) with distilled water. Methyl Green dye (Sigma Aldrich) was prepared in molar concentrations and varied from  $5 \times 10^{-5}$  to  $5 \times 10^{-3}$  mol/L per 50 mL in solution of one molar of perchloric acid, maintained at 293 – 333 K in a thermostatic water bath.

### Weight Loss Measurement

The weight of carbon steel specimens before and after immersion was determined by using an analytical balance with the precision of 0.1 mg. The immersion time for the WL measurement was 2 h. All experiments were in triplicates and the illustrated data are presented in mean values of the obtained results.

The following equations were used to calculate corrosion rate (CR), inhibition efficiency (IE) and surface coverage ( $\theta$ ) [21]:

$$CR = (w_b - w_a)/S t \quad (1)$$

$$IE = 100x(CR' - CR)/CR' \quad (2)$$

$$\theta = IE/100 \quad (3)$$

Where:  $w_b$  and  $w_a$  are the sample mass (g) before and after immersion in the test solution, respectively; S is the total area of the specimen (cm<sup>2</sup>); t is the exposure time (h); and CR' and CR are corrosion rates of CS samples in the absence and presence of inhibitor (g cm<sup>-2</sup> h<sup>-1</sup>), respectively.

### Design of Experimental Strategy

Optimization of inhibition efficiency (IE) and corrosion rate (CR) is reached by using the response surface methodology (RSM) based on two methods for estimating the model's coefficients: PLS (partial Least Squares) [22, 23] and MLR (Multiple Linear Regression) [24]. RSM is a technique to determine design factor settings to improve or optimize the performance of the response. It combines design of experiments, regression analysis, and optimization methods in a general-purpose strategy to optimize the expected value of a stochastic response. In particular,

the empirical relationships between the response and the factors are investigated using the central composite face-centered design (CCF) [25, 26].

The behavior of the system is explained by the following quadratic equation:

$$y = a_0 + \sum_i a_i X_i + \sum_i a_{ii} X_i^2 + \sum_{ij} a_{ij} X_i X_j + \varepsilon \quad (4)$$

Where: y is the matrix of responses;  $X_1, X_2, X_3, \dots, X_n$  are the independent coded variables;  $a_0$  is the intercept;  $a_i, a_{ii}$  and  $a_{ij}$  represent the linear pure quadratic and interaction regression coefficients; and  $\varepsilon$  is the statistical random error term.

The implementation of experimental design is important to identify the significant factors that impact the efficiency of the tested inhibitor and the corrosion rate. In our study, optimum experimental conditions based on central composite face-centered design 2<sup>3</sup> were used. The experimental design and statistical analysis were performed using MODDE Software Version 9.1. A standard RSM based on PLS (Partial Least Squares) was used to determine the individual and interactive effects of the process on independent factors, i.e., concentration of inhibitor ( $X_1$ ), temperature ( $X_2$ ), and immersion time ( $X_3$ ). On other hand, inhibition efficiency and corrosion rate (Y) were selected as response functions. The variable range was divided into three levels (-1, 0, +1), as shown in Table 1. Response (Y) was fitted to a general function indicating the interaction between dependent and independent variables by following the quadratic (second degree) polynomial equation given by Equation 4.

## RESULTS AND DISCUSSION

### Effect of Concentration and Temperature on Inhibition Efficiency

The weight loss measurements were determined in 1 M HClO<sub>4</sub> with different concentrations of MG dye (from  $5 \times 10^{-5}$  to  $5 \times 10^{-3}$  mol/L) for two hours of immersion time. Fig. 1 shows the variation of calculated inhibition efficiency values as a function of logarithmic concentration of the inhibitor. It is obvious from the data of Fig. 1 that inhibition efficiency increased with increasing

**Table 1.** The real and coded experimental design range parameter levels for corrosion inhibition of MG dye

Factors	Names	Units	Levels		
			Low (-1)	Middle (0)	High (+1)
$X_1$	Concentration	(mol/L)	$5.0 \times 10^{-5}$	$2.5 \times 10^{-3}$	$5.0 \times 10^{-3}$
$X_2$	Temperature	(°C)	20	40	60
$X_3$	Time	(h)	1	2	3

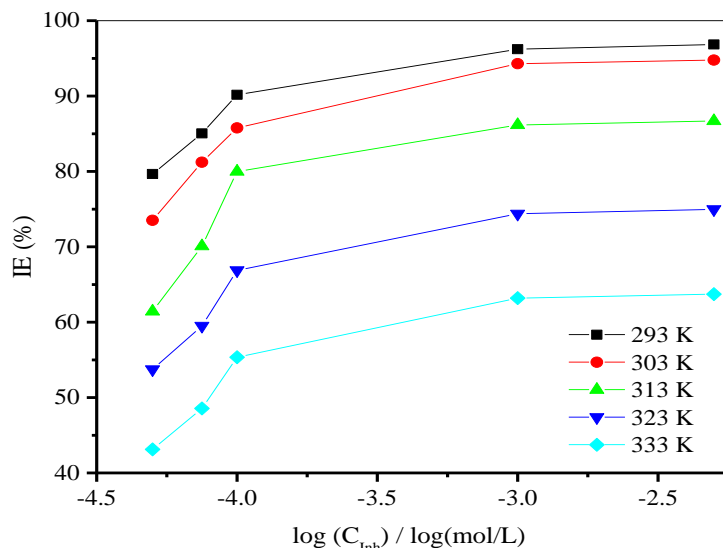


**Figure 1.** The relation between IE (%) and log (C<sub>inh</sub>) of MG dye at different temperatures at 2 hrs

concentration of the inhibitor because of the availability of a large number of adsorption sites brought about by molecules of MG dye. Moreover, it was found that at a given inhibitor concentration, inhibition efficiency decreased in general with increasing temperature. At higher temperatures, MG was desorbed from CS surface. Methyl Green dye was found to work properly at lower temperatures, with poor inhibition capabilities at higher temperatures. At  $5 \times 10^{-3}$  mol/L, inhibition efficiency was observed to be stable for all studies after  $1 \times 10^{-3}$  mol/L. This behavior was attributed to the saturation of inhibitor molecules on CS surface. The maximum IE (%) was obtained at the optimum concentration of  $1 \times 10^{-3}$  mol/L at 303 K.

### Effect of Immersion Time

Time duration of the surface exposed to the corrosive environment directly affects the rate of corrosion. The variation of weight loss of CS immersed in different time intervals up to 24 hours in 1 M HClO<sub>4</sub> solution at 303 K in the absence and presence of MG dye is shown in Fig. 2. From Fig. 2, we observe that the two curves are almost linear (with and without MG dye); this implies that the metal surface was free of insoluble corrosion products. So, we can deduce that this quantity was almost constant from the first hour of immersion, which allows us to say that immersion time has no significant effect on the corrosion inhibition of CS in 1.0 M HClO<sub>4</sub> by MG dye for the optimum concentration of the inhibitor.

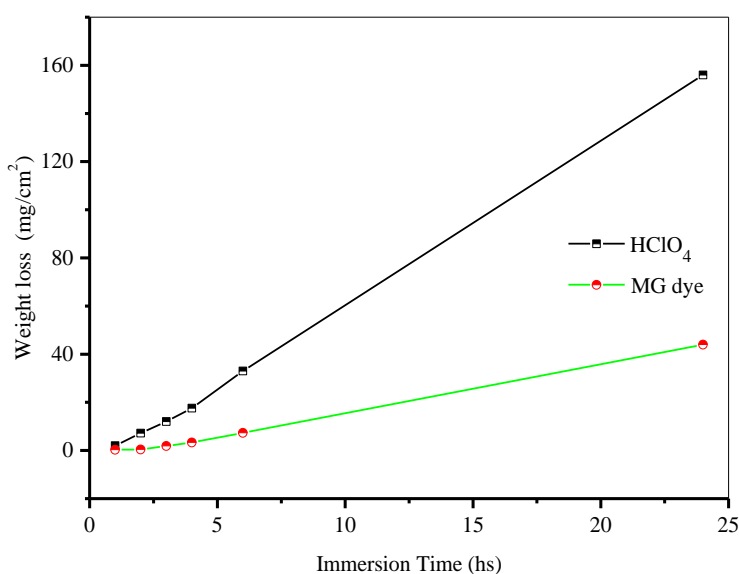


**Figure 2.** Weight loss-time for CS in 1.0 M HClO<sub>4</sub> in the absence and presence of  $1 \times 10^{-3}$  mol/L of MG dye at 303 K

**Thermodynamic and Kinetic Parameters**

The efficiency of the inhibitor may decrease due to the absence of protective film formed or removed as a result of localized erosion corrosion [27]. It has been reported elsewhere that for the acid corrosion of CS, the logarithm of the corrosion rate is a linear function of 1/T, where T is the absolute temperature following Arrhenius eq. (5) and the transition state eq. (6) [28, 29].

$$\ln(\text{CR}) = \ln(A) + -E_a/RT \tag{5}$$

$$\ln(\text{CR}/T) = [\ln(R/Nh) + \Delta S_a/R] - \Delta H_a/RT \tag{6}$$

The change in Gibbs energy can be deduced at

313 K by Eq. 7.

$$\Delta G_a = \Delta H_a - T\Delta S_a \tag{7}$$

Where,  $E_a$  is the apparent activation energy,  $\Delta S_a$  is the entropy of activation,  $\Delta H_a$  is the enthalpy of activation,  $R$  is the gas constant (8.314 J/molK),  $N$  is the Avogadro number ( $6.022 \times 10^{23} \text{ mol}^{-1}$ ), and  $h$  is Planck's constant ( $6.626 \times 10^{-34} \text{ J/s}$ ).

$E_a$  could be obtained by plotting  $\ln(\text{CR})$  against  $1/T$ , as shown in Fig. 3. Moreover, from Eq. 6, a plot of  $\ln(\text{CR}/T)$  against  $1/T$  should give a straight line with a slope of  $(-\Delta H_a/R)$  and an intercept of  $(\ln(R/Nh) - \Delta S/R)$ , as shown in Fig. 4. The calculated parameters of  $E_a$ ,  $\Delta H_a$ ,  $\Delta S_a$ , and  $\Delta G_a$  are given in Table 2.

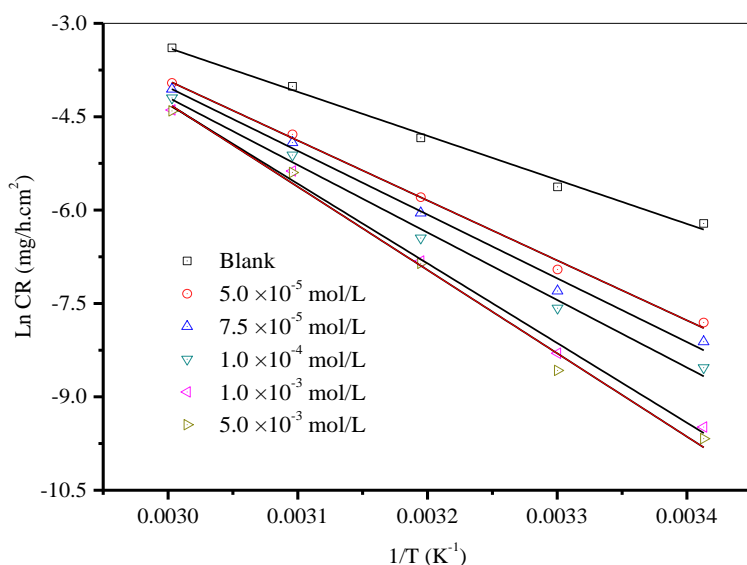


**Figure 3.** Arrhenius plots for the corrosion of CS in 1 M HClO<sub>4</sub> medium in the absence and presence of different concentrations of MG dye

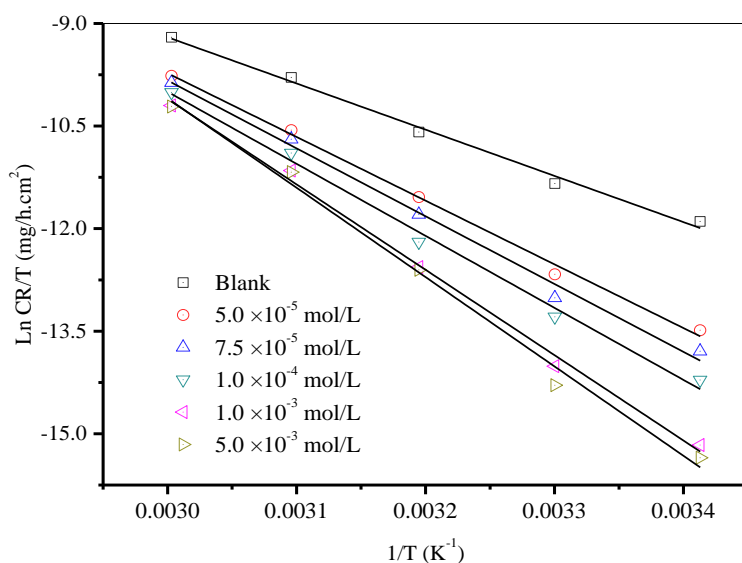


**Figure 4.** Alternative Arrhenius plots for CS dissolution in 1 M HClO<sub>4</sub> medium in the absence and presence of different concentrations of MG dye

**Table 2.** The thermodynamic activation functions of CS dissolution in 1 M HClO<sub>4</sub> without and with different concentrations of MG dye by applying Arrhenius and transition state plots

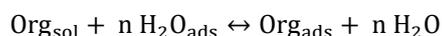
C <sub>inh</sub> (mol/L)	R <sup>2</sup>	E <sub>a</sub> (kJ/mol)	ΔH <sub>a</sub> (kJ/mol)	ΔS <sub>a</sub> (J/molK)	ΔG <sub>a</sub> (313K) (kJ/mol)
-	0.992	58.79	56.20	-105.44	89.20
5.0 × 10 <sup>-5</sup>	0.995	80.06	77.46	-46.02	91.86
7.5 × 10 <sup>-5</sup>	0.991	85.09	82.49	-31.81	92.45
1.0 × 10 <sup>-4</sup>	0.992	90.17	87.58	-17.91	93.18
1.0 × 10 <sup>-3</sup>	0.995	106.41	103.82	-29.91	113.18
5.0 × 10 <sup>-3</sup>	0.991	111.24	108.65	-44.48	122.57

The addition of MG dye to the acid solution increased E<sub>a</sub> and the extent of the increase was proportional to the inhibitor concentration, indicating that the energy barrier for the corrosion reaction increased with MG dye concentration. The average value of the difference between activation energy and enthalpy change (E<sub>a</sub> – ΔH) was 2.59 kJ/mol for all concentrations, which was the exact value of the product of gas constant and the average temperature of the experiment (313 K). That is E<sub>a</sub> – ΔH = RT. This result indicated that the corrosion process was a unimolecular reaction with the evolution of hydrogen gas. The entropy of activation in the absence and presence of MG dye was large and negative. The high negative value of ΔS<sub>a</sub> in the absence of inhibitor implies that the activated complex was the rate-determining step, rather than the dissociation step. The positive signs of enthalpy of activation reflect the endothermic nature of the steel dissolution process. The positive values of free Gibbs energy mean a non-spontaneous corrosion reaction and it increased with increasing the concentration of inhibitor. Moreover, the higher values of ΔG<sub>a</sub> of the process in the inhibitor's presence when compared to that in its absence were attributed to its physisorption, while the opposite is the case with chemisorption.

### Adsorption Isotherm

Adsorption isotherms provide information about the interaction of adsorbed molecules not only among themselves but also their interactions with a metal surface. The process of adsorption is influenced by various factors like the nature and charge of the metal, and the type of aggressiveness and chemical structure of the inhibitor (aromaticity, functional groups, possible steric effects, etc.). The adsorption of dye molecules at the metal solution interface reduces the corrosion rate and it is considered as a substitution adsorption process where an organic

compound from the aqueous media displaces the water molecules associated with the surface (H<sub>2</sub>O<sub>ads</sub>).



Where, 'n' is the number of water molecules replaced by the adsorption of one inhibitor molecule.

In general, chemisorption process involves sharing or transfer of charges from the inhibitor molecules to the metal surface to form a coordinate type of a bond, on the other hand the proceeding of physisorption requires the presence of both electrically charged metal surface and charged species in the bulk of the solution.

Corrosion inhibition of CS in the presence of different inhibitor concentrations has been studied to the adsorption on the CS surface, and this was generally confirmed from the fit of the experimental data to different adsorption isotherms.

Langmuir model is based on the hypothesis that each site of metal surface has adsorbed species (Equation 8) [13]:

$$C_{\text{Inh}}/\theta = 1/K_{\text{ads}} + C_{\text{Inh}} \quad (8)$$

Where, θ is the surface coverage by inhibitor molecule, C is the concentration, and K<sub>ads</sub> is the equilibrium constant (L/mol) for the adsorption-desorption process.

The plots of C<sub>inh</sub>/θ against C<sub>inh</sub> (Fig. 5) yielded straight lines with slope values equal to unity, indicating that the inhibitor under study obeyed the Langmuir adsorption isotherm.

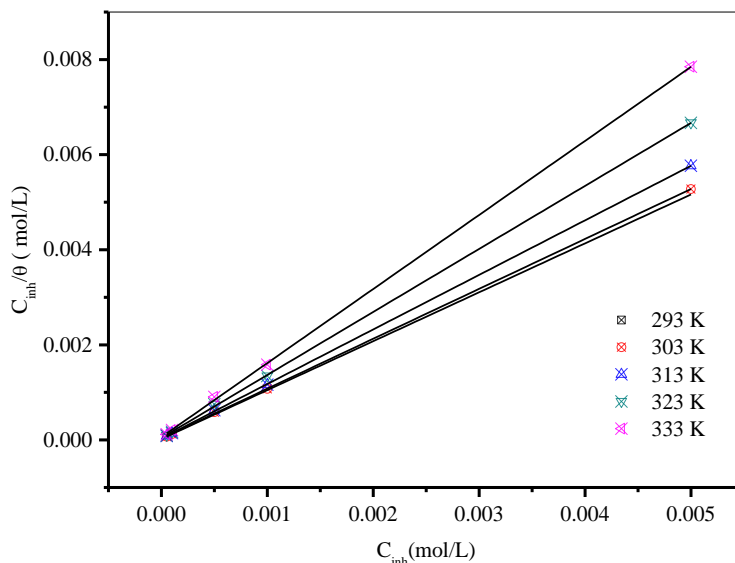


**Figure 5.** Langmuir isotherm for the adsorption of MG dye on CS in 1 M HClO<sub>4</sub>

**Table 3.** Thermodynamic parameters for the adsorption of MG dye in 1 M HClO<sub>4</sub> solution on C-Steel at different temperatures

T	R <sup>2</sup>	K <sub>ads</sub> (m <sup>3</sup> /mol)	ΔH <sub>ads</sub> (kJ/mol)	ΔS <sub>ads</sub> (J/mol K)	ΔG <sub>ads</sub> (kJ/mol)
293	1	52.27		50.53	-36.24
303	1	34.99		49.61	-36.47
313	1	34.03	-21.44	51.64	-37.60
323	1	23.99		50.85	-37.86
333	1	16.74		49.86	-38.04

The free energy of the adsorption of an inhibitor on CS surface can be evaluated with the following equation [29]:

$$\Delta G_{ads} = -RT \ln(55.5 K_{ads}) \tag{9}$$

Where, R is the gas constant (J/mol K) and T is the absolute temperature (K). The constant value of 55.5 is the concentration of water in the solution (mol/L).

The results of the present studies at 293 K to 333 K indicated that the mechanism of adsorption of the inhibitor onto CS surface is better obeyed by the Langmuir adsorption isotherm (Table 3).

The negative value of the heat of adsorption of -21.44 kJ/mol indicates that the adsorption of the inhibitor on CS was an exothermic process. The adsorption equilibrium constants are positive, indicating the feasibility of the adsorption of the inhibitor to the metal surface. The high value of the

equilibrium constant at lower temperature reflects the high adsorption ability of MG dye on CS surface [30]. This result further confirms the trend obtained for activation energy. Generally, if the values of ΔG<sub>ads</sub> are more than -20 kJ/mol, then the physisorption mechanism is favored. Whereas, if the values of ΔG<sub>ads</sub> are -40 kJ/mol or lower, then the adsorption process is chemisorption. As shown in Table 3, the ΔG<sub>ads</sub> values are negative and between -20 kJ/mol and -40 kJ/mol. This result indicates that adsorption of MG dye on CS surface was spontaneous, feasible, and occurred according to possible mixture of physisorption and chemisorption mechanism

### Regression Analysis and Optimization

The experiments performed for optimization of IE and CR are presented in Table 4, which were analyzed using analysis of variance. The technique for coding the corrosion parameters is clarified. The final equations in terms of actual factors are presented in Eqs. (10) and (11).

$$y_{IE} (\%) = 85.101 + 7.494 X_1 - 12.421 X_2 - 1.525 X_3 - 5.038 X_1^2 - 3.232 X_2^2 - 2.156 X_3^2 + 0.986 X_1 X_2 - 0.595 X_1 X_3 + 1.249 X_2 X_3 \tag{10}$$

$$y_{CR} = 1.02076 \cdot 10^{-3} - 1.0848 \cdot 10^{-3} X_1 + 5.82913 \cdot 10^{-3} X_2 + 1.39063 \cdot 10^{-4} X_3 + 1.01021 \cdot 10^{-3} X_1^2 + 2.52387 \cdot 10^{-3} X_2^2 + 6.90914 \cdot 10^{-4} X_3^2 - 1.0559 \cdot 10^{-3} X_1 X_2 - 4.90627 \cdot 10^{-5} X_1 X_3 + 3.65838 \cdot 10^{-5} X_2 X_3 \quad (11)$$

**Table 4.** The experimental design of the coded and real factors with the corrosion rate and inhibition efficiency

Exp. N°	Run Order	Factors						Responses	
		$X_1$ : Concentration		$X_2$ : Temperature		$X_3$ : Time		IE (%)	CR (g.cm <sup>-2</sup> h <sup>-1</sup> )
		Coded	Real	Coded	Real	Coded	Real		
1	9	-1	5.0×10 <sup>-5</sup>	-1	20	-1	1	79.58	8.168×10 <sup>-5</sup>
2	11	1	5.0×10 <sup>-3</sup>	-1	20	-1	1	96.61	1.356×10 <sup>-5</sup>
3	5	-1	5.0×10 <sup>-5</sup>	1	60	-1	1	43.07	1.839×10 <sup>-2</sup>
4	13	1	5.0×10 <sup>-3</sup>	1	60	-1	1	63.11	1.192×10 <sup>-2</sup>
5	8	-1	5.0×10 <sup>-5</sup>	-1	20	1	3	75.49	5.882×10 <sup>-4</sup>
6	15	1	5.0×10 <sup>-3</sup>	-1	20	1	3	85.21	3.549×10 <sup>-4</sup>
7	16	-1	5.0×10 <sup>-5</sup>	1	60	1	3	42.93	1.889×10 <sup>-2</sup>
8	1	1	5.0×10 <sup>-3</sup>	1	60	1	3	63.04	1.223×10 <sup>-2</sup>
9	12	-1	5.0×10 <sup>-5</sup>	0	40	0	2	61.43	3.05×10 <sup>-3</sup>
10	14	1	5.0×10 <sup>-3</sup>	0	40	0	2	86.69	1.05×10 <sup>-3</sup>
11	10	0	2.5×10 <sup>-3</sup>	-1	20	0	2	96.27	1.343×10 <sup>-4</sup>
12	17	0	2.5×10 <sup>-3</sup>	1	60	0	2	63.33	1.232×10 <sup>-2</sup>
13	6	0	2.5×10 <sup>-3</sup>	0	40	-1	1	83.57	1.08×10 <sup>-3</sup>
14	2	0	2.5×10 <sup>-3</sup>	0	40	1	3	80.61	1.61×10 <sup>-3</sup>
15	7	0	2.5×10 <sup>-3</sup>	0	40	0	2	86.31	1.08×10 <sup>-3</sup>
16	4	0	2.5×10 <sup>-3</sup>	0	40	0	2	86.31	1.08×10 <sup>-3</sup>
17	3	0	2.5×10 <sup>-3</sup>	0	40	0	2	86.31	1.08×10 <sup>-3</sup>

The values of correlation, adjusted, and predicted R-squares (Table 5) show that the model equations are predictive and can reliably be useful for sampling data within the experimental range of parameters. For both CR and IE attested to the reliability of the analysis with 95 percent confidence level. The Q2 value is a measure of how well the model will work for future predictions. Q2 should be greater than 0.1 for a significant model, and greater than 0.5 for a good model. Moreover, for a good model (Q2 > 0.9), the model validity can

still be low because of high test sensitivity or extremely good replicates. From Table 5, the Q2 obtained for IE and CR is close to 0.9, which indicates a good model in this study.

Both IE (%) and CR indicated high dependence and good correlation between the observed and predicted values of the responses. These results of the relationship between the experimental and predicted values can be confirmed by the good agreement described in Fig. 6 [31].

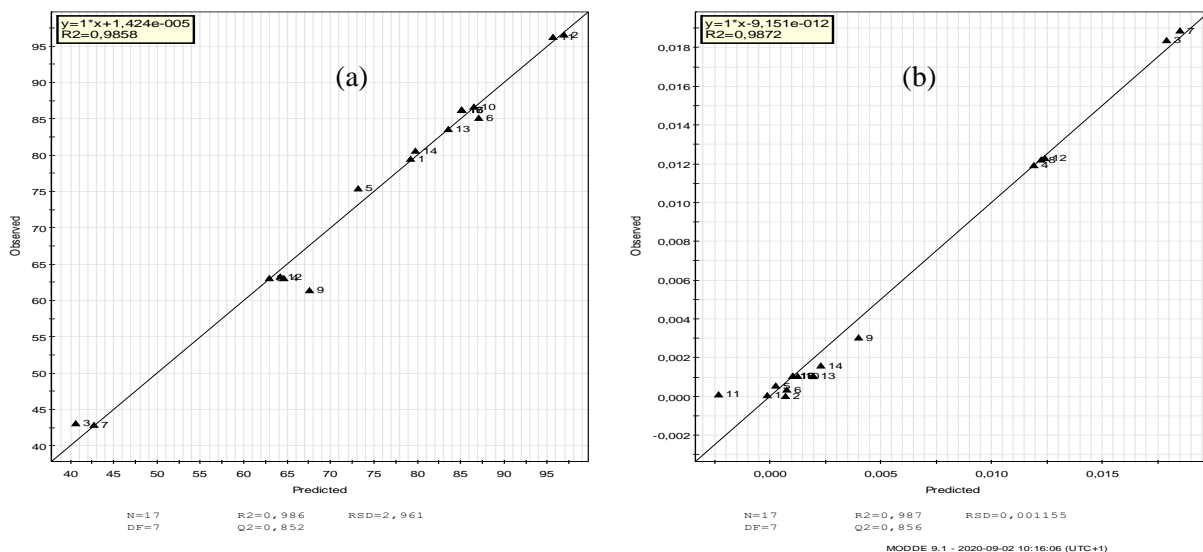


**Figure 6.** Comparison of responses of predicted values and experimental data of (a) inhibition efficiency and (b) corrosion rate

**Table 5.** Analysis of variance for corrosion rate and inhibition efficiency of CS in 1 M HClO<sub>4</sub>

	Inhibition efficiency (%)	Corrosion rate (g/h.cm <sup>2</sup> )
R <sup>2</sup>	0.986	0.987
Adj. R <sup>2</sup>	0.968	0.971
Q2	0.852	0.856
R.S.D	2.961	1.155 10 <sup>-3</sup>
Conf. level	0.95	0.95

To observe the optimum zone of the two responses, we plotted the response surfaces. The response surface plots (Fig. 7) and the 4D contour plots, the projection of the response surfaces as 4-dimensional planes, (Fig. 8 and 9) were made to verify the effects of the three parameters on IE (%) and CR. This analysis gives a better understanding of the effects of variables and their interactions on

responses. It also allows determining any value of the response without even doing an experimental study. From Fig. 8, as inhibitor concentration increased from minimum to maximum concentration, IE (%) increased with the decrease of temperature. For any fixed amount of MG dye in the system, IE increased with time, but higher for higher concentrations of inhibitor.

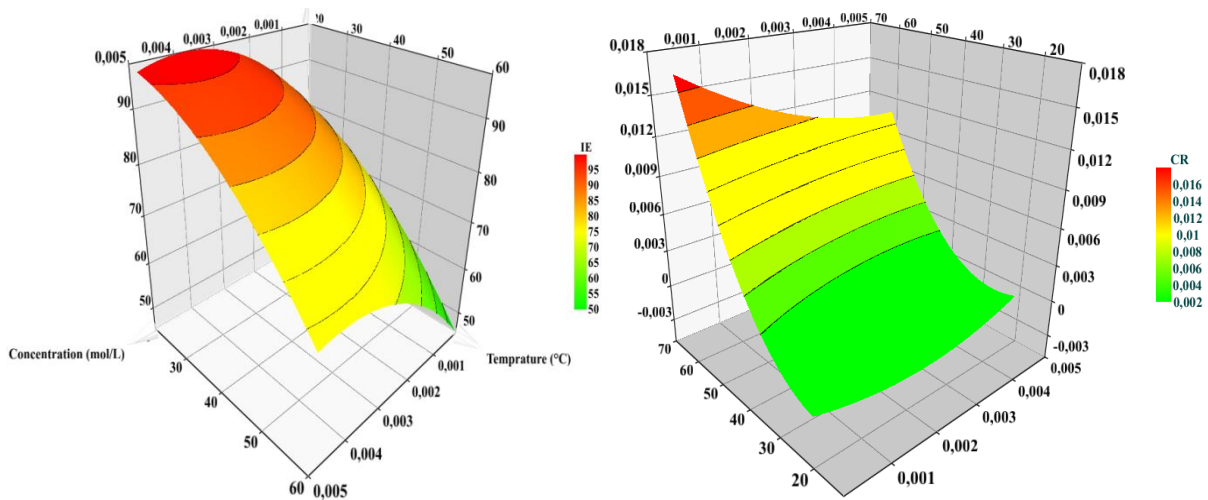


**Figure 7.** Response surface plots of the effects of temperature and inhibitor concentration on inhibition efficiency (left) and corrosion rate at two hours (right)

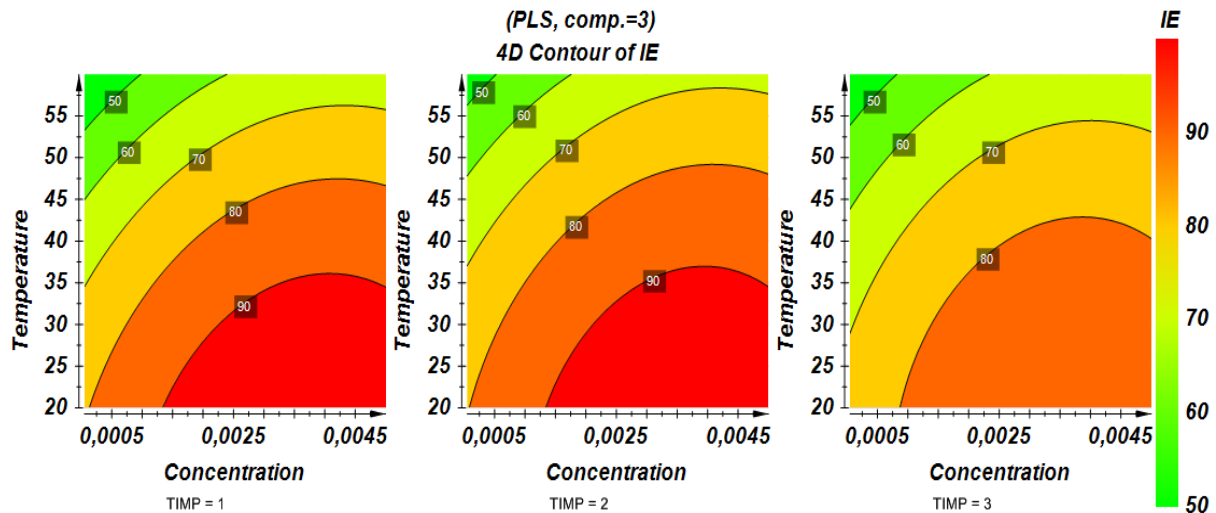


**Figure 8.** 4D Contour plots of effects of temperature, concentration, and time on inhibition efficiency

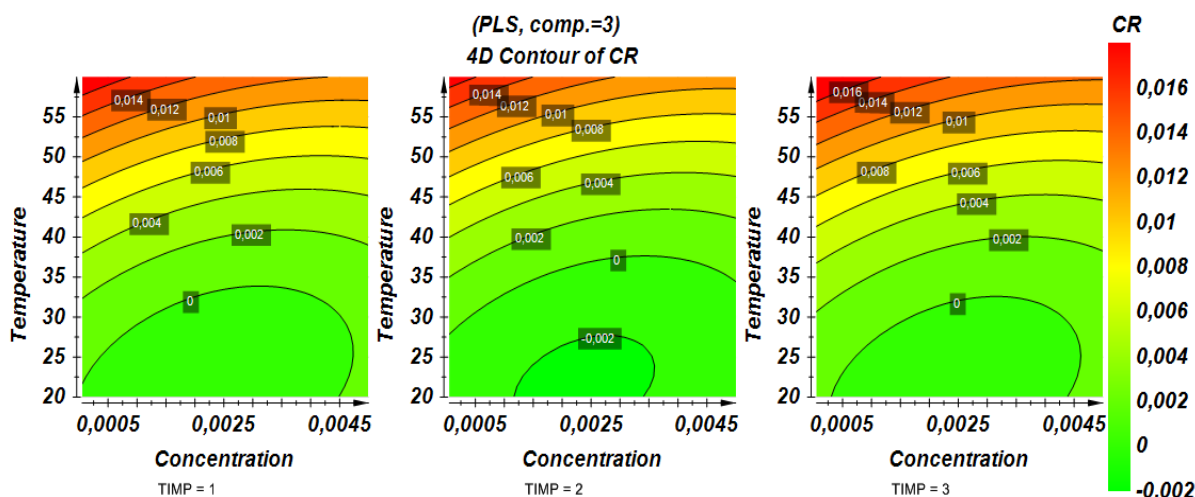


Figure 9. 4D Contour plots of effects of temperature, concentration, and time on corrosion rate

### CONCLUSION

The experimental design has enabled us to study inhibition efficiency and corrosion rate with different factors such as MG dye concentration, immersion time and temperature, and through a limited number of carefully selected tests, to get a description of the studied response behavior within the experimental area and thus determine experimental conditions that maximize the efficiency of inhibition. In this regard, the obtained efficiency was 97.45% for the treatment at 20.5°C for two hours, for a quantity of inhibitor of  $3.66 \times 10^{-3}$  mol/L. The negative value of Gibbs free energy is an indication of a spontaneous adsorption process. Both chemisorption and physisorption are proposed from the values of activation energy and changes in Gibbs free energy. The corrosion process was inhibited by adsorption of the molecules of Methyl Green dye on carbon steel surface following Langmuir adsorption isotherm.

### REFERENCES

- Loto, R. T., Loto, C. A., Joseph, O. O., Olanrewaju, G. (2016) Adsorption and corrosion inhibition properties of thiocarbanilide on the electrochemical behavior of high carbon steel in dilute acid solutions. *Results. Phys.*, **6**, 305–314.
- Rahal, H. T., Abdel-Gaber, A. M., Younes, G. O. (2016) Inhibition of steel corrosion in nitric acid by sulfur containing compounds. *Chem. Eng. Commun.*, **203**, 435–445.
- Attar, T., Larabi, L., Harek, Y. (2014) The Inhibition effect of potassium iodide on the corrosion of pure iron in sulfuric acid. *Adv. Chem.*, **2014**, 1–5.
- Attar, T., Benchadli, A., Choukchou-Braham, E. (2019) Corrosion inhibition of carbon steel in perchloric acid by potassium iodide. *Inter. J. Adv. Chem.*, **7**, 35–41.
- Ko, X., Sharma, S. (2017) Adsorption and self-assembly of surfactants on metal-water interfaces. *J. Phys. Chem. B.*, **121**, 10364–10370.
- Al-Moghrabi, R. S., Abdel-Gaber, A. M., Rahal, H. T. (2019) Corrosion Inhibition of Mild Steel in Hydrochloric and Nitric Acid Solutions Using Willow Leaf Extract. *Prot. Met. Phys. Chem. Surf.*, **55**, 603–607.
- Oguzie, Emeka E. (2009) Inhibiting effect of crystal violet dye on aluminum corrosion in acidic and alkaline media. *Chem. Eng. Commun.*, **196**, 591–601.
- Karumalaiyan, P., Perumal, K., Alagan, S. (2018) Evaluation of chromotrope FB dye as corrosion inhibitor using electrochemical and theoretical studies for acid cleaning process of petroleum pipeline. *Surf.Interfaces.*, **12**, 50–60.
- El Boraie, N., Halim, S., Ibrahim, M. (2018) Effective corrosion inhibition of mild steel in acidic medium using inexpensive kermes natural dye: experimental and quantum chemical study. *Anti-Corros.Method. M.*, **65**, 626–636.
- Sivakumara, V., Velumania, K., Rameshkumar, S. (2018) Colocid Dye - A Potential Corrosion Inhibitor for the Corrosion of Mild Steel in Acid Media. *Mater. Res.*, **21**, 1–10.
- Özkır, D. (2019) The Electrochemical Variation of a Kind of Protein Staining and Food Dye as a New Corrosion Inhibitor on Mild Steel in Acidic Medium. *Int. J. Electrochem.*, **2019**, 1–11.
- Mallikarjuna, N. M., Keshavayya, J., Prasanna,

- M. (2020) Synthesis Characterization and Anti-corrosion Behavior of Novel Mono Azo Dyes Derived from 4,5,6,7-Tetrahydro-1,3-benzothiazole for Mild Steel in Acid Solution. *J. Bio. Tribo. Corros.*, **6**, 1–7.
13. Attar, T., Benchadli, A., Messaoudi, B., Benhadria, N., Choukchou-Braham, E. (2020) Experimental and Theoretical Studies of Eosin Y Dye as Corrosion Inhibitors for Carbon Steel in Perchloric Acid Solution. *Bull. Chem. React. Eng. Catal.*, **15**, 454–464.
  14. Benhachem, F. Z., Attar, T. (2019) Comparison studies for the removal of a basic dye from aqueous solution using coffee residues and waste tea. *Inter. J. Adv. Chem.*, **7**, 97–103.
  15. Benhachem, F. Z., Attar, T., Bouabdallah, F. (2019) Kinetic study of adsorption methylene blue dye from aqueous solutions using activated carbon from starch. *Chem. Rev. Lett.*, **2**, 33–39.
  16. Yang, J., Qiu, K. (2011) Experimental design to optimize the preparation of activated carbons from herb residues by vacuum and traditional  $\text{ZnCl}_2$  chemical activation. *Ind. Eng. Chem. Res.*, **50**, 4057–4064.
  17. Ghoreishi, S. M., Saeidinejad, F., Behpour, M., Masoum, S. (2015) Application of multivariate optimization to electrochemical determination of methyl dopa drug in the presence of diclofenac at a nanostructured electrochemical sensor. *Sensor Actuat B-Chem.*, **221**, 576–585.
  18. Garcia-Manrique, P., Matos, M., Gutierrez, G., Estupinan, O. R., Blanco-Lopez, M. C., Pazos, C. (2016) Using factorial experimental design to prepare size-tuned nanovesicles. *Ind. Eng. Chem. Res.*, **55**, 9164–9175.
  19. Afzalkhah, M., Masoum, S., Behpour, M., Naeimi, H., Reisi-Vanani, A. (2017) Experimental and Theoretical Investigation of Inhibition Efficiency of 2-(2-Hydroxyphenyl)-benzothiazole Using Impedance Spectroscopy, Experimental Design, and Quantum Chemical Calculations. *Ind. Eng. Chem. Res.*, **56**, 9035–9044.
  20. Al-Shamkhani, M. T., Ateik, Adnan A. (2018) Use of Experimental Designs to Evaluate the Influence of Ziziphus Leaves Extracts as a Corrosion Inhibitor for Mild Steel in (3.5 M) NaCl. *Int. J. Appl. Eng. Res.*, **13**, 7416–7423.
  21. Attar, T., Larabi, L., Harek, Y. (2014) Inhibition effect of potassium iodide on the corrosion of carbon steel (XC 38) in acidic medium. *Inter. J. Adv. Chem.*, **2**, 139–142.
  22. Wold, N. K. (1992) Analysis of mixture data with partial least square. *Chemom. Intell. Lab. Syst.*, **14**, 57–69.
  23. Wold, H. (1975) Soft Modelling by latent variables; the nonlinear iterative partial least squares approach. Perspectives in Probability and Statistics, Gani, J. (Ed), (Papers in honour of M. S. Bartlett). London : Academic Press.
  24. Weisberg, S. (1985) Applied Linear Regression, 2nd edition, John Wiley, New York, 324.
  25. Rosales, E., Sanroman, M. A., Pazos, M. (2012) Application of central composite face-centered design and response surface methodology for the optimization of electro-Fenton decolorization of Azure B dye. *Envir. Sci. Pollu. Reach.*, **19**, 1738–1746.
  26. Maran, J. P., Manikandan, S., Nivetha, C. V., Dinesh, R. (2017) Ultra sound assisted extraction of bioactive compounds from Nephelium-lappaceum L. fruit peel using central composite face centered response surface design. *Arab. J. Chem.*, **10**, 1145–1157.
  27. Khan, P. F., Shanthi V., Babu, R. K., Muralidharan S., Barik, R. C. (2015) Effect of benzo-triazole on corrosion inhibition of copper under flow conditions. *J. Envir. Chem. Eng.*, **3**, 10–19.
  28. Khouri, S. J. (2015) Titrimetric study of the solubility and dissociation of benzoic acid in water: effect of ionic strength and temperature. *Am. J. Analyt. Chem.*, **6**, 429–436.
  29. Attar, T., Larabi, L., Harek, Y. (2014) Corrosion inhibition of cold rolled steel in 0.5 M  $\text{H}_2\text{SO}_4$  by potassium iodide. *Der Pharma Chemica.*, **6**, 181–186.
  30. Benchadli, A., Attar, T., Choukchou-Braham, E. (2019) Inhibition of Carbon Steel Corrosion in Perchloric Acid Solution by Povidone Iodine. *Phys. Chem. Res.*, **7**, 837–848.
  31. Wu, J., Doan, H. (2005) Disinfection of recycled red-meat processing wastewater by ozone. *J. Chem. Technol. Biotechnol.*, **80**, 828–833.